Testing scale models of *hydroreactor* stream accelerators – Experimental Results

António José Arsénio dos Santos Costa
e-mail: antonio.costa@peehr.pt / URL: www.peehr.pt
PEEHR, Lda, Rua Nova Nº 2, Areia Branca, 2530-065 Lourinhã, Portugal

Keywords: *Hydroreactor* stream accelerator, scale model, raft, axial flow, increase in head.

Abstract

The purpose of this paper, is to present experimental results obtained by testing a number of scale models of *hydroreactor* stream accelerators for stream energy extraction, with differences on shape, aiming at obtaining the shape influence on efficiency of the model and to describe design approaches to an optimised model to be adopted on the real scale.

Introduction

Hydroreactor stream accelerators consist on conduits of optimised design, that sustain immersed in the streams, containing a channel formed by an inlet compression zone, an intermediate zone of narrower cross section (gorge) where in the absence of flow constraints (such as a stream turbine), the water flows with a velocity higher than the outside stream velocity and finally by an exhaust divergent part where a suction effect is generated by diffusion of the inside flow and depression of the outside stream nearby the channel outlet. In the channel narrower zone (gorge) works a low head axial flow turbine, that drives by transmission means a low rpm generator logged inside an impervious chamber located on the space between the inside and outside surfaces, not affecting the hydrodynamics of the flow though the *hydroreactor*. An increase in head is obtained with these stream accelerators, resulting in a power flux density in the narrower channel zone that is higher than the outside free stream power flux density. They have the effect of very low head dam in addition to the normal kinetic stream strength. The use of *hydroreactor* stream accelerators promotes the increase of the number of profitable sites.

Description of the measurements

Several scale models with different geometries, where tested in a real environment. The experiments were performed using models with dimensions higher than the ones supported in laboratory, all defined by a channel narrower diameter of 300 mm, in order to reduce the scale effects and thus increasing the reliability of the measurements, and to allow testing with small size turbine models. For safety reasons, the experiments were conducted in still water (Bay of Peniche Port), fixing to a raft the scale models immersed, and simulating the streams effect with the raft in motion dragging the scale models under water.

The efficiency of a model can be measured by the obtained increase in head for a specific stream velocity. In order to determine the models efficiency, several tests were performed, measuring as a function of the raft velocity relatively to water (equivalent to the stream velocity), the velocity of the flow and the static pressure inside the narrower channel zone, in the absence of flow constraints (free condition) and with 3 predefined loadings (L1, L2 and L3) providing 58%, 72% and 82% area obstruction to flow. For each conduit model, the following variables were measured as functions of the raft velocity (equivalent to the stream velocity *Vc*):

Fig. 1: View of raft during experiments.

- The flow velocity *Vt* through the narrower channel zone, in the absence of flow constraints;
- The flow velocity *Vt* through the narrower channel zone, measured before the loading offering resistance to flow (for loadings L1, L2 and L3);
- The static pressure *P* measured transversally to the flow direction, in the narrower channel zone, before the loading offering resistance to flow (for loadings L1, L2 and L3);

Several plots are shown to compare the performance of the tested models:

I-) The Ratio *Vt/Vc* between the flow velocity *Vt* through the narrower channel zone in the absence of flow constraints and the outside stream velocity *Vc*, as a function of *Vc*.

II-) The increase in head $+\Delta H$ obtained by using a specific duct model, as a function *Vc*, calculated in the absence of flow constraints as $+\Delta H = Vt^2/(2g) - Vc^2/(2g)$.

III-) The Ratio *Vt/Vc* between the flow velocity *Vt* through the narrower channel zone, measured before the loading (for loadings L1, L2 and L3) and the outside stream velocity *Vc*, as a function of *Vc*.

IV-) The static pressure *P* in the narrower channel zone before the loading as a function of *Vc*.

V-) The static pressure *P* in the narrower channel zone before the loading as a function of the flow velocity *Vt* at the same point.

VI-) The available head $-\Delta H$ before the loading (that corresponds to the loss of head at the loading assuming that the static pressure and velocity after loading are null), being $-\Delta H = Vt^2/(2g) + P/\gamma$ (where g is the gravity acceleration and γ the water specific weight density), as a function of the flow velocity *Vt*.

Presentation and Discussion of Experimental Results

Figures A1.1, A1.2, A1.5, A1.6, A1.9, A1.10, A1.13 and A1.14 of Appendix A1 present performance data I and II, respectively for Models B1, C1, B2, C2, B3, B4, A1 and A2. According to these plots, the ratio *Vt/Vc* is, in the absence of flow constraints, almost steady for the range of tested stream velocities. Table 1 shows characteristic values of the ratio *Vt/Vc* in the absence of flow constraints, for the several duct models tested.

Table 1: Ratio *Vt/Vc* in the absence of flow constraints

Model	A1	A2	B1	C1	B2	C2	B3	B4
Vt/Vc%	140 %	125 %	110 %	105 %	115 %	115 %	120 %	115 %

According to the results we may conclude that, the creation of depression at outlet helps to increase the power flux through the channel narrower zone. Models B1 and C1 consist on a simple duct having a highly concentrating inlet funnel not providing any mechanisms to generate significant depression in order to compensate inlet concentration. The performance of Models B2 and C2 are similar to Model B4, meaning that the use of a simple plate (with a diameter wider than the duct external surface) to create more depression is as efficient as having a geometry with symmetric inlet and outlet zones. Models B2 and C2 have the disadvantage of presenting higher resistance to the streams implying the use of stronger fixating infrastructures. Model B3 presents a divergent zone not too short to avoid interfering overlap between the inside flow and outside stream vortexes nor too long to avoid the existence of a hydrostatic zone between the inside flow and outside stream vortexes, but with optimum length to guarantee auxiliary rotation between inside flow and outside stream vortexes. It was verified on practice that an exaggerated divergent zone would decrease the performance of the models. Thus, the outlet divergent zone should be of optimum size and shape in order to maximize efficiency. Model A1 has a divergent zone with the same capacity as Model B3, if we despise the spaces in the divergent zone of Model B3 with hydrostatic fluids. Beside this,

Model A1 presents an external surface slightly inclined and free of obstacles to facilitate creation of depression nearby the outlet section. The slope of this surface is more accentuated in Model A1 than in Model A2, what means that more depression is generated at the outlet for Model A1. Model A1 presents also slightly higher capacities for the inlet concentration and outlet diverging zones than Model A2.

The accelerating conduit model to be used in real scale should have an optimized shape, being similar to Model A1 that is according to the performed experiments the more efficient model among all the tested duct models. According to graphic A1.13, the flow velocity *Vt* through the narrower channel zone is in the absence of flow constraints about 40% higher than the velocity *Vc* of the outside free stream, corresponding to an increase in head $+\Delta H$ of 200 mm for a stream velocity *Vc* of 2 m/s (4 knots).

Figures A2.1, A2.3 and A2.5 show the characteristics of *P* and of *Vt/Vc* as a function of *Vc* for Model A1 respectively with loadings L1, L2 and L3. Figures A2.2, A2.4 and A2.6 show the characteristics of *P* and of *Vt/Vc* as a function of *Vc* for Model A2 respectively with loadings L1, L2 and L3. According to these graphics:

The verified ratio *Vt/Vc* is for a specific stream velocity and loading value, higher for model A1 than for model A2.

The verified ratio *Vt/Vc* is for specific Model, as much higher as less obstructing is the loading located in the narrower channel zone, being *Vt/Vc (L1) > Vt/Vc (L2) > Vt/Vc (L3).*

As more obstructing is the loading, higher is the stream velocity *Vc* beyond which the water starts to flow through the inside channel. Graphics of figures A 2.5 and A 2.6 show that the verified stream velocity beyond which starts to flow water through inside the channel is with loading L3, about 1m/s (2 knots) for Model A1 and about 1.25 m/s (2.5 knots) for Model A2. Graphics of figures A 2.3 and A 2.4 show that this value tends to about 0,5 m/s (1 knot) for Model A1 and to about 0,75 m/s (1.5 knot) for Model A2 with loading L2. With no loading, the stream velocity beyond which the water starts to flow through the channel tends to 0 m/s.

Figures A2.7, A2.9 and A2.11 show for Model A1 the characteristics of the static pressure *P* measured before the loading and of the available head $-\Delta H$ before the loading as functions of *Vt*, respectively with loadings L1, L2 and L3. Figures A2.8, A2.10 and A2.12 show for Model A2, the characteristics of the transversal pressure *P* measured before the loading and of the available head $-\Delta H$ before the loading, as functions of *Vt*, respectively with loadings L1, L2 and L3.

According to these graphics the available head $-\Delta H$ before a specific loading is higher for Model A1 than for Model A2, meaning that Model A1 is more efficient than Model A2.

Table 2: Typical values with several loadings in the channel narrower zone

Vc	**1,25 m/s (2,5 knots)**				**1,75 m/s (3,5 knots)**			
Loading	**No**	**L1**	**L2**	**L3**	**No**	**L1**	**L2**	**L3**
***Vt/Vc* (%)**	140%	35 %	25%	8%	135%	45%	35%	20%
***Vt* (m/s)**	1,75	0,44	0,31	0,1	2,36	0,79	0,61	0,35
***P* (Pa)**	-	1450	1500	1600	-	2200	2300	2500
$-\Delta H$ (mm)	156	153	155	160	285	252	250	255

Graphics from Appendix A2 show that for a specific stream velocity value *Vc*, the available head before the loading given by $-\Delta H = Vt^2/(2g) + P/\gamma$ is almost independent of the applied loading (L1, L2 or L3), being equivalent to the verified available head in this zone without any flow constraints $-\Delta H = Vt^2/(2g)$. This is only valid, considering not extremely obstructing loadings that do not imply rejection of energy flow through the channel. The flow of water through the conduit channel tends to be cancelled for totally obstructing loadings. Table 2 shows values verified for Model A1, considering two stream velocity values *Vc* (1,25 m/s and 1,75 m/s).

Conclusions

It was proved in practice, that for the more efficient tested accelerator model (Model A1), to be adopted in reality, the flow velocity *Vt* through the channel narrower zone is in the absence of flow constraints about 40% higher than the velocity *Vc* of the outside free stream, meaning an increase in the available head of about 200 mm for a stream velocity of 2 m/s (4 knots). It was also verified, that for *hydroreactor* stream accelerators, the ratio *Vt/Vc* between the velocity in the channel narrower part *Vt* and the outside stream velocity *Vc* is in the absence of flow constraints almost constant for the range of typical stream velocities.

Graphic of figure 2, shows for the best tested model (Model A1), to be adopted in reality, characterised in the absence of flow constraints by a constant ratio *Vt/Vc* of 1.4, the estimated increase in head $+\Delta H$ and available power *P* as functions of the outside stream velocity *Vc*, considering conduit narrower channel diameters of 1m, 1.5m and 2m.

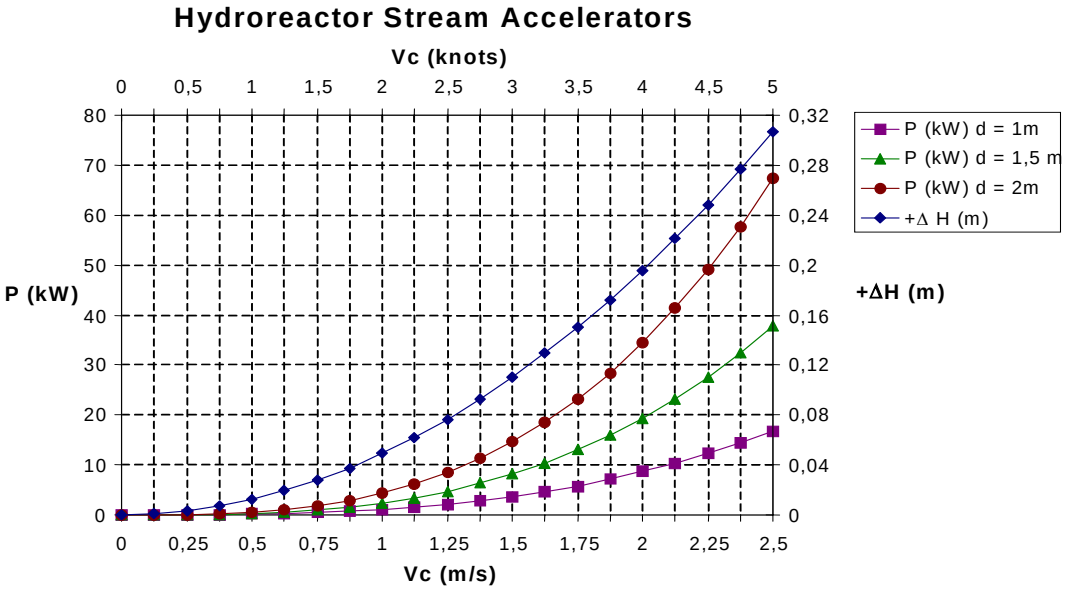

Figure 2: Available power *P* and increase in head $+\Delta H$ with the stream velocity

A system with a platform fitted on a mast, supporting two *hydroreactor* stream accelerators, generates for a 2m/s (4 knot) stream, about 2 x 10 kW, 2 x 20 kW or 2 x 35 kW power, considering respectively accelerator narrower channel diameters of 1m, 1,5m or 2m.

In conclusion this technology has potential for conversion of kinetic energy from streams, because *hydroreactor* stream accelerators create an increase in head with relation to the normal kinetic stream strength, promoting the increase of the number of profitable sites.

Acknowledgments: To A. Sarmento, professor of Fluid Mechanics and Renewable Energies at the Mechanical Department of the Higher Technical Institute IST in Lisbon and responsible for the Wave Energy Centre, for his contribution on the revision and planning of measurements executed by the author.

Appendix A1

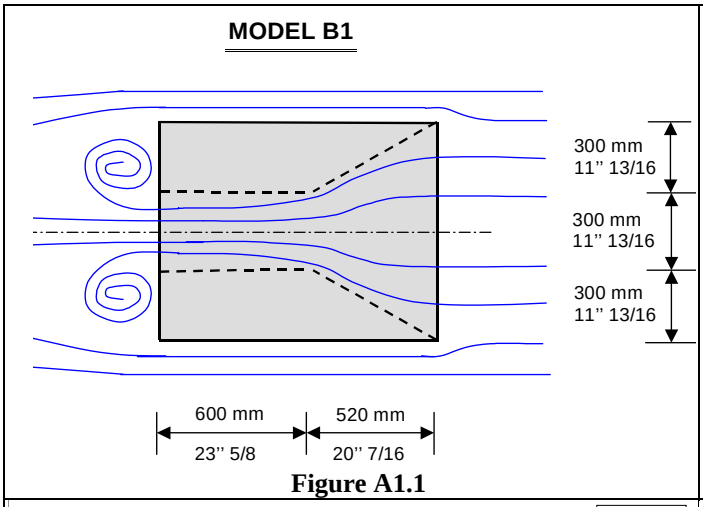

Figure A1.1

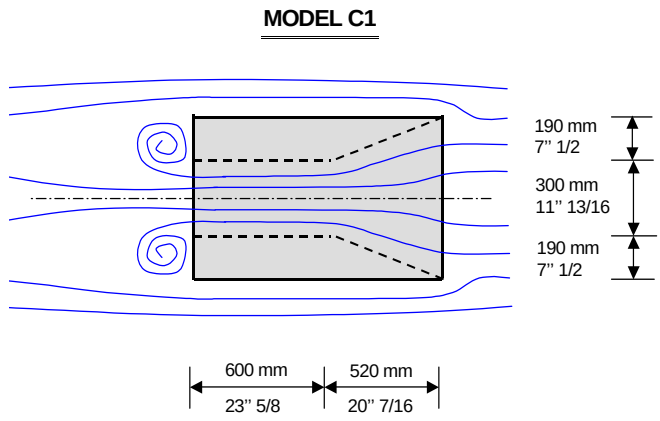

Figure A1.2

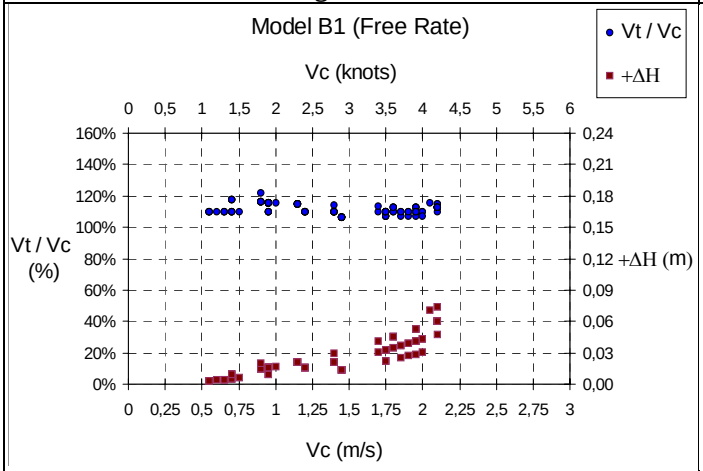

Figure A1.3

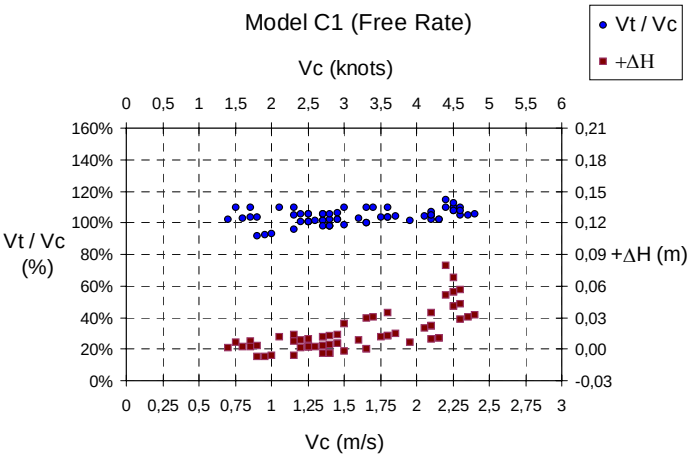

Figure A1.4

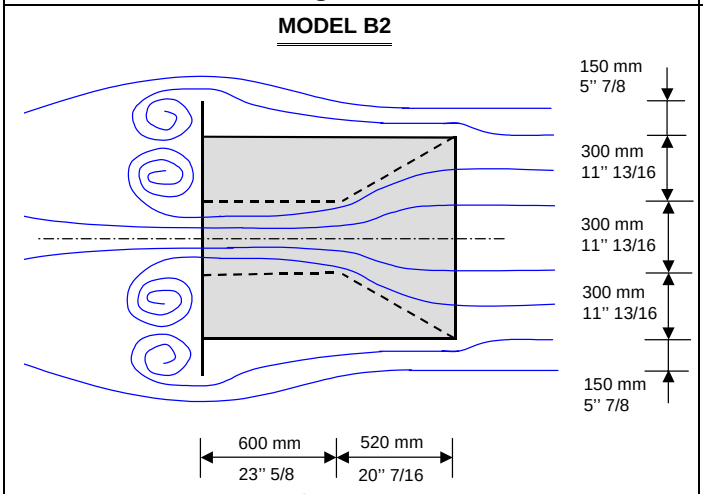

Figure A1.5

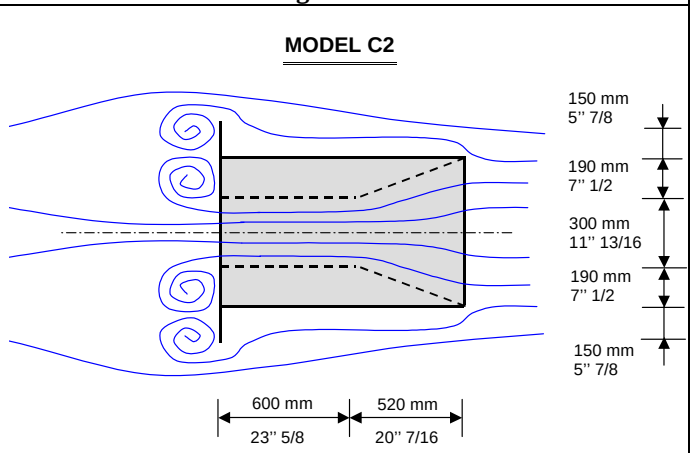

Figure A1.6

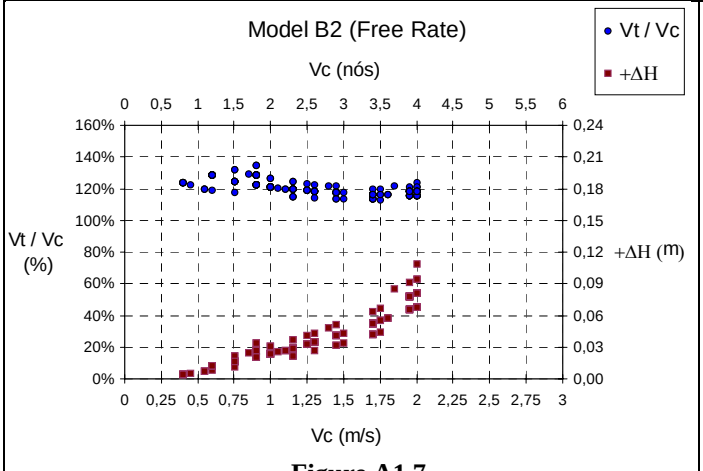

Figure A1.7

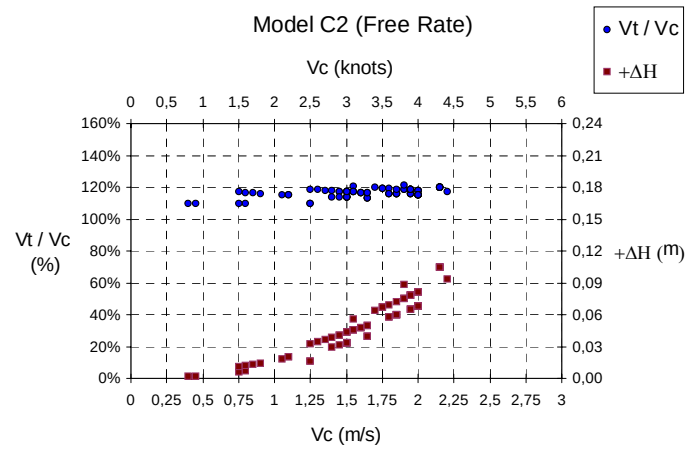

Figure A1.8

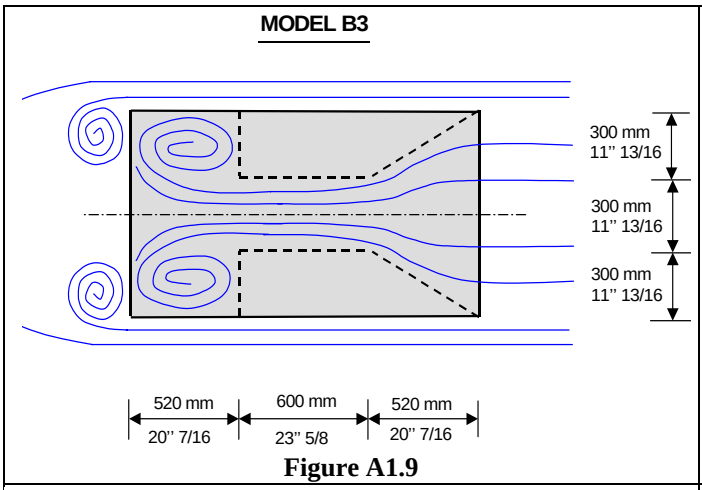

Figure A1.9

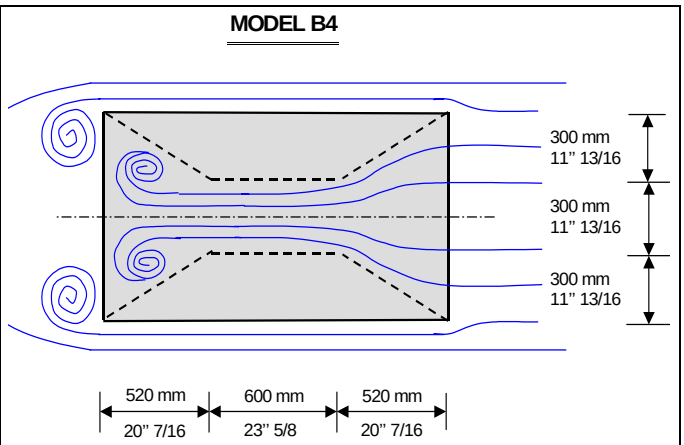

Figure A1.10

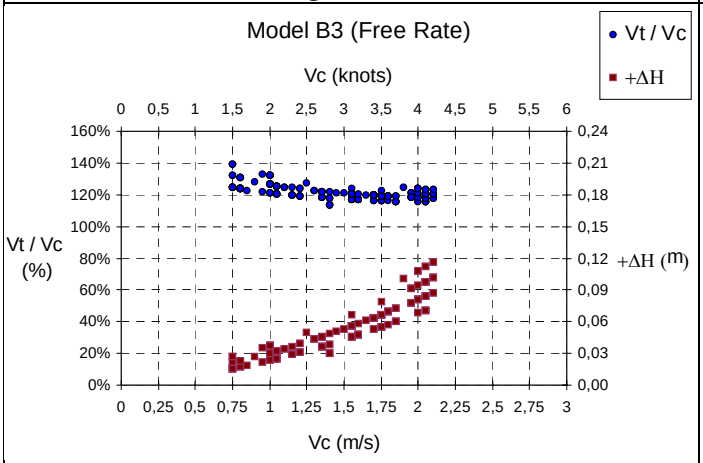

Figure A1.11

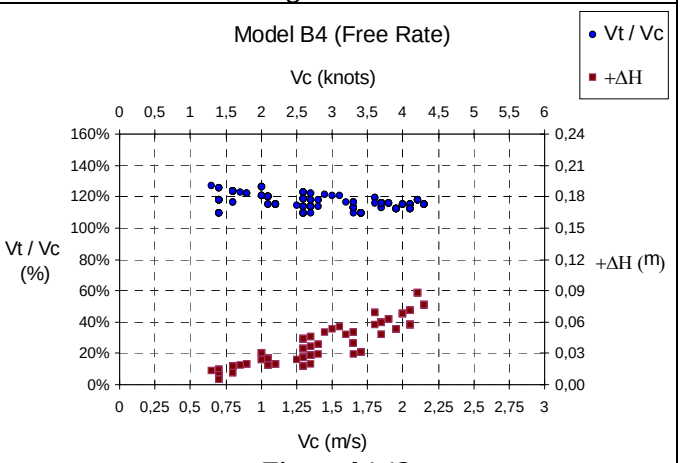

Figure A1.12

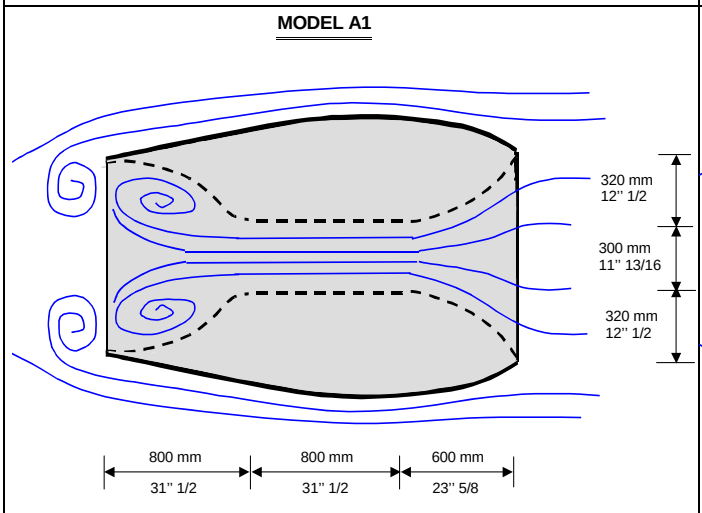

Figure A1.13

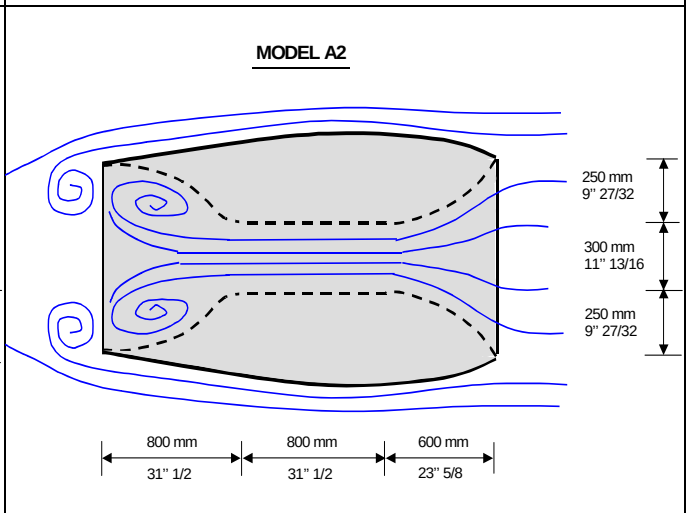

Figure A1.14

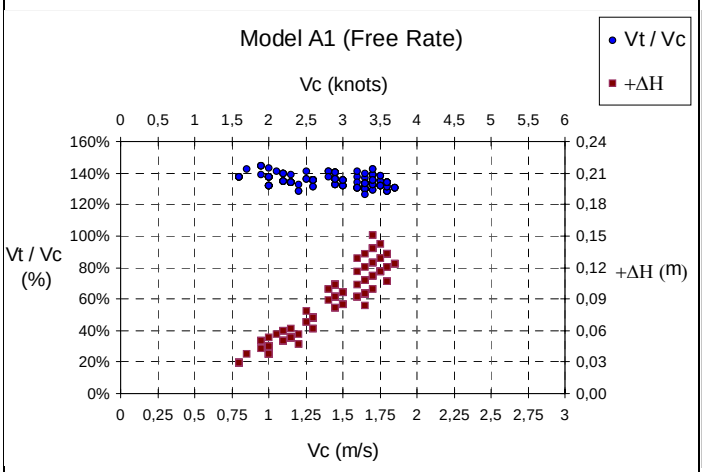

Figure A1.15

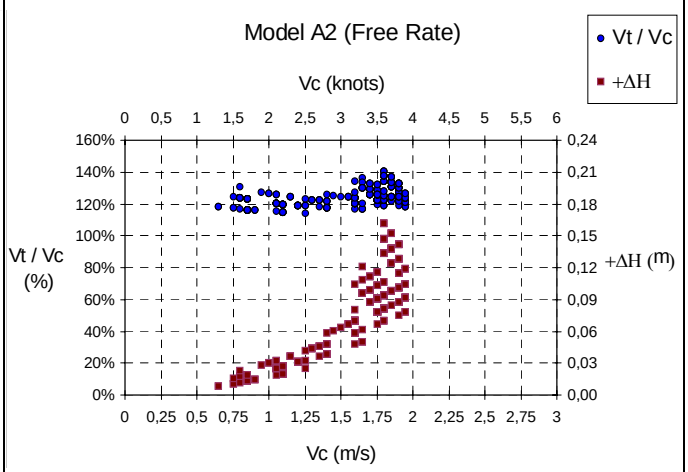

Figure A1.16

Appendix A2

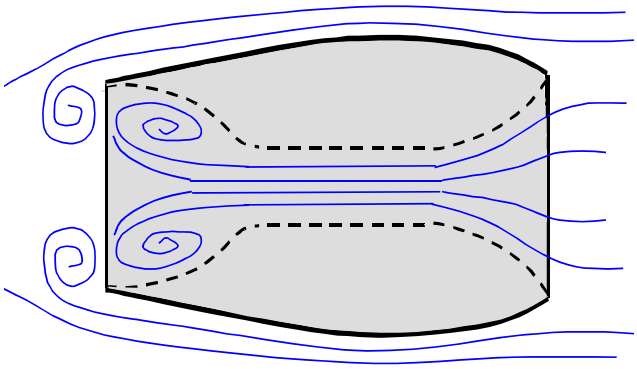

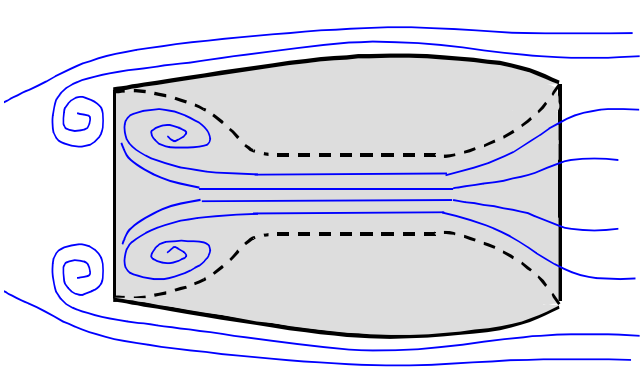

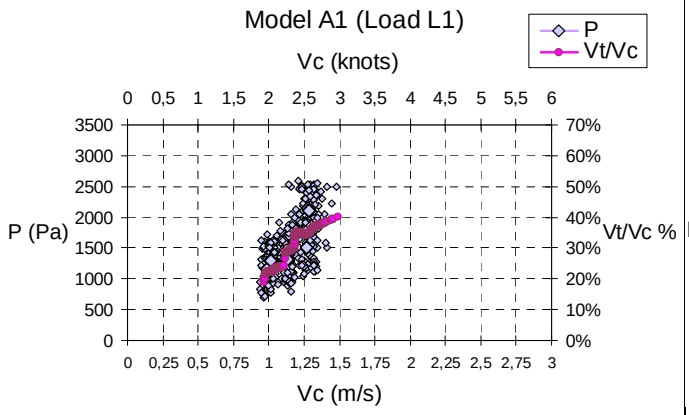

Figure A2.1

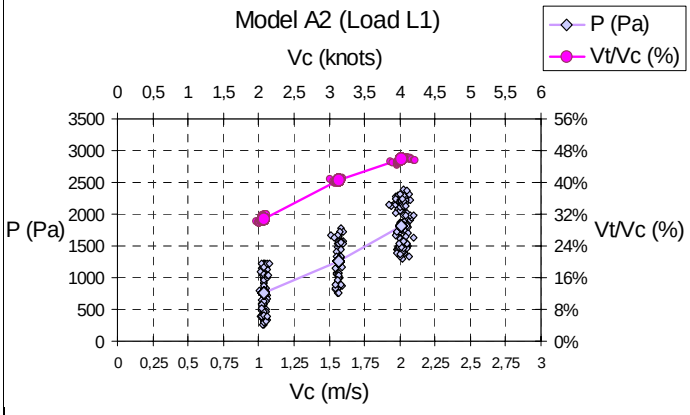

Figure A2.2

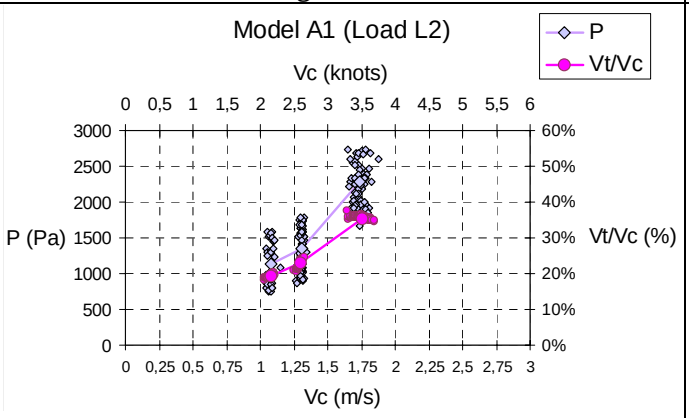

Figure A2.3

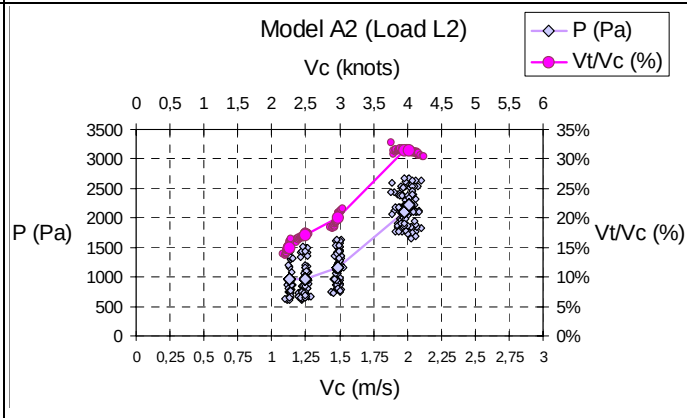

Figure A2.4

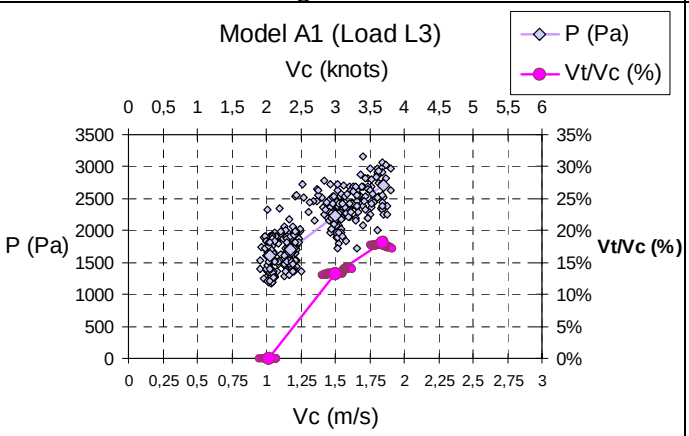

Figure A2.5

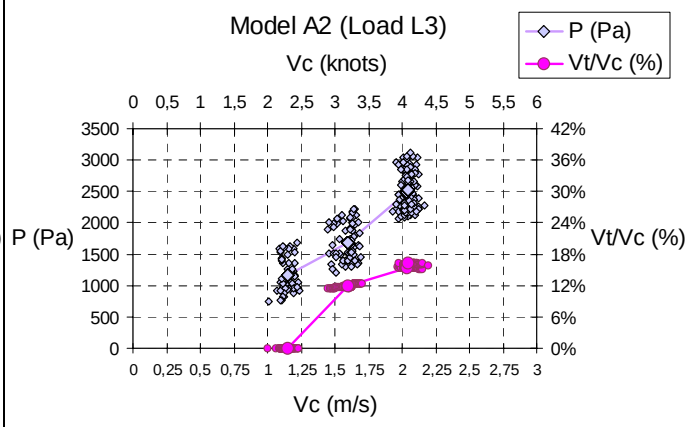

Figure A2.6

MODEL A1

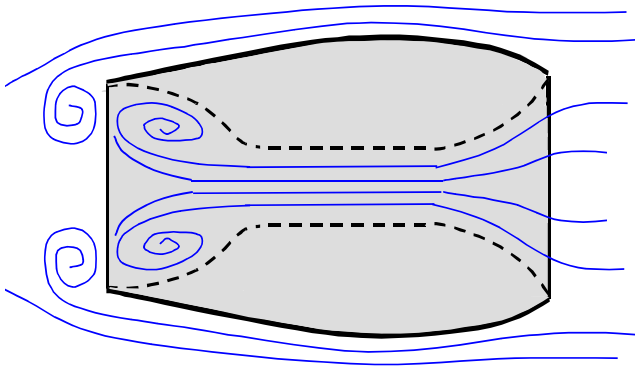

MODEL A2

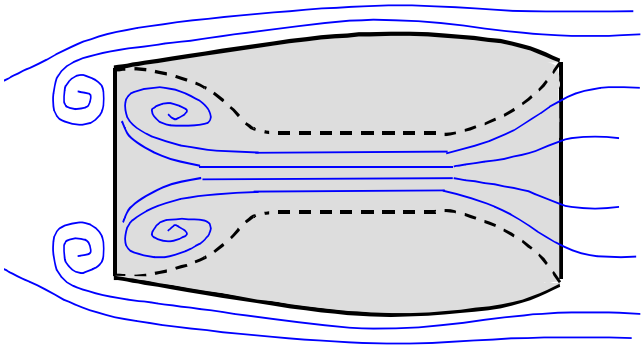

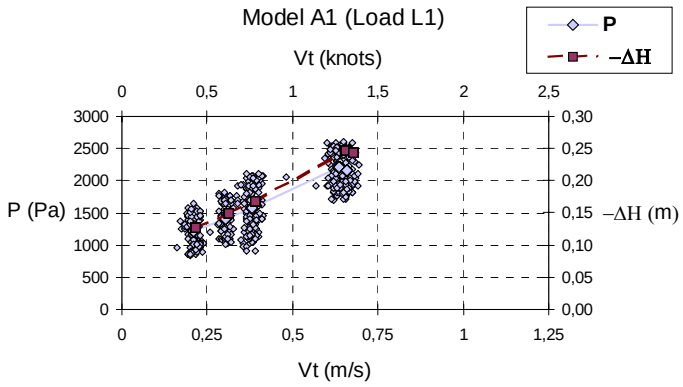

Figure A2.7

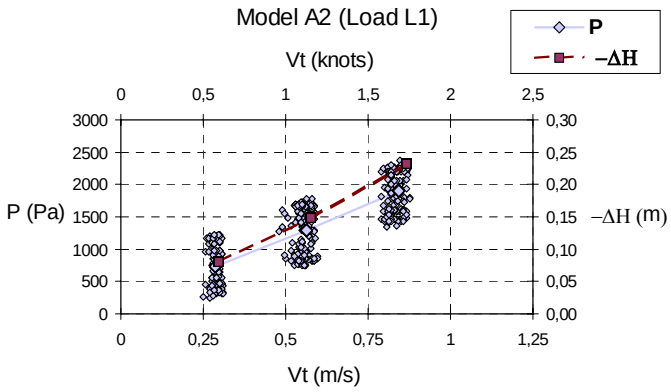

Figure A2.8

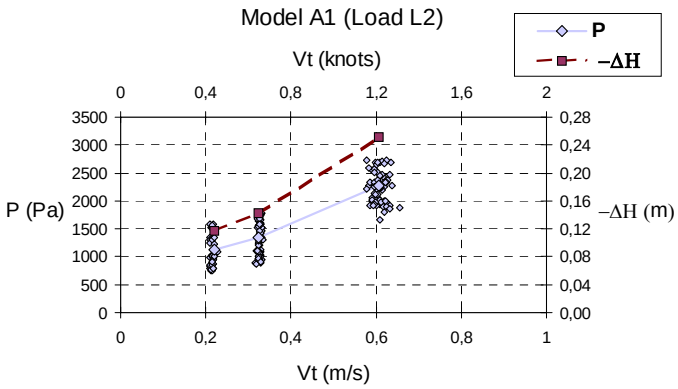

Figure A2.9

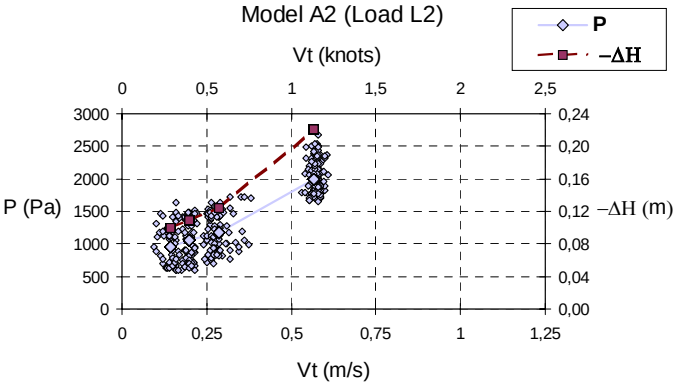

Figure A2.10

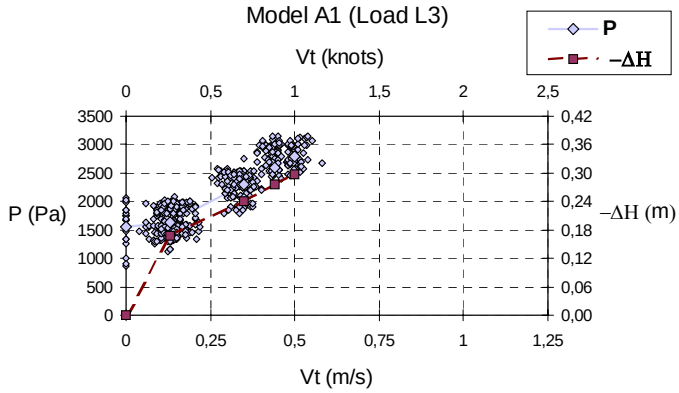

Figure A2.11

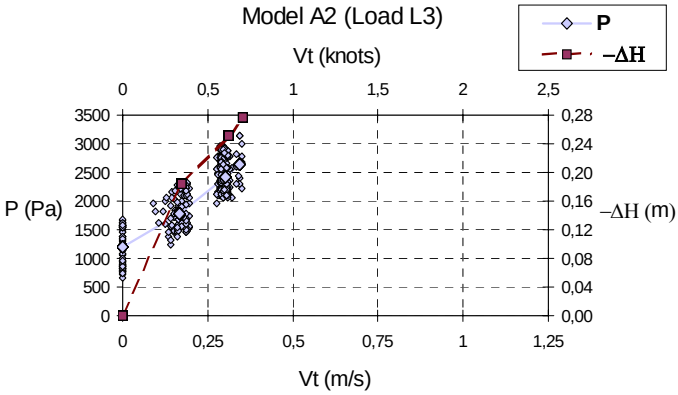

Figure A2.12